

Geophysical Research Letters



RESEARCH LETTER

10.1029/2021GL093291

Key Points:

- A reference mid-tropospheric temperature time series was developed using advanced satellite microwave sounder observations in stable orbits
- The reference time series can detect the mid-tropospheric temperature trends with an accuracy better than 0.01 Kelvin/Decade
- The mid-tropospheric temperature trends observed from the reference time series are 0.230 ± 0.134 Kelvin/Decade during 2002–2020

Supporting Information:

Supporting Information may be found in the online version of this article.

Correspondence to:

C.-Z. Zou,
Cheng-Zhi.Zou@noaa.gov

Citation:

Zou, C.-Z., Xu, H., Hao, X., & Fu, Q. (2021). Post-millennium atmospheric temperature trends observed from satellites in stable orbits. *Geophysical Research Letters*, 48, e2021GL093291. <https://doi.org/10.1029/2021GL093291>

Received 11 MAR 2021
 Accepted 8 JUN 2021

Post-Millennium Atmospheric Temperature Trends Observed From Satellites in Stable Orbits

Cheng-Zhi Zou¹ , Hui Xu² , Xianjun Hao³ , and Qiang Fu⁴

¹Center for Satellite Applications and Research, NOAA/NESDIS, College Park, MD, USA, ²ESSIC/CISESS, University of Maryland, College Park, MD, USA, ³Environmental Science and Technology Center, College of Science, George Mason University, Fairfax, VA, USA, ⁴Department of Atmospheric Sciences, University of Washington, Seattle, WA, USA

Abstract We develop a post-millennium mid-tropospheric temperature time series from continuous observations by advanced microwave sounders onboard satellites in stable sun-synchronous orbits. Such observations have high radiometric stability and do not experience diurnal sampling changes over time, allowing us to develop merged time series from multiple satellites with an accuracy better than 0.012 Kelvin/Decade. With such high accuracy, the resulting time series can be used as a reference measurement of climate variability and trends in atmospheric temperatures. The warming rate from this time series for the atmospheric layer between surface and 10 km is 0.230 ± 0.134 Kelvin/Decade during the period from 2002 to 2020, which is $\sim 14\%$ higher than the existing satellite microwave sounder datasets. Our finding provides new insight on trend differences among microwave sounder temperature data sets developed by different research groups, and is also helpful in reconciling trend differences between satellite observations and climate model simulations.

Plain Language Summary Atmospheric temperature time series developed from satellite microwave sounder observations has been extensively used in climate change monitoring and verifying climate model simulations of climate change. However, uncertainties exist in the satellite merged products and their resulting atmospheric temperature trends, mainly caused by diurnal sampling changes over time and instrument calibration errors. Satellite products developed by different research groups produced different atmospheric temperature trends, undermining the capability of using satellite observations in global change monitoring. Here we develop a reference time series from 2002 to present using advanced satellite microwave sounder observations in stable sun-synchronous orbits for the detection of global mid-tropospheric temperature trends with accuracy better than 0.012 Kelvin/Decade. This high accuracy in trend detection was achieved because diurnal sampling drifting errors do not exist for satellites in stable orbits and that these measurements have high radiometric stability. This reference measurement is expected to help reconcile differences in climate trend comparisons among different satellite products and between climate model simulations and satellite observations during the post-millennium periods. It may also be helpful in the development of atmospheric temperature time series with a better accuracy for satellites before the millennium when used as a reference.

1. Introduction

Changes in the atmospheric temperature are one of the central indicators of global warming. Spaceborne satellites have been playing a vital role in measuring global atmospheric temperature trends during the past few decades (Christy et al., 2000, 2003; Spencer & Christy, 1992a, 1992b; Mears & Wentz, 2009, 2016; Mears et al., 2003; Po-Chedley et al., 2015; Spencer et al., 2017; Wentz & Schabel, 1998; Zou & Wang, 2011; Zou et al., 2006). These measurements were made from the Microwave Sounding Unit (MSU) and its follow-on advanced MSU (AMSU) onboard the National Oceanic and Atmospheric Administration (NOAA), National Aeronautics and Space Administration (NASA), and European Organization for the Exploitation of Meteorological Satellites (EUMETSAT) polar-orbiting satellites. The MSU/AMSU instruments passively measure the upwelling radiances from the 50- to 60-GHz absorption band of the atmospheric oxygen in discrete frequency channels (Kidwell, 1998). The radiance measured by each frequency channel comes from a different thick layer of the atmosphere, depending on the strength of the absorption at that frequency. The relative contribution of temperatures at individual levels to the measured layer temperature is represented by a vertical weighting function, which is typically a bell-shaped curve peaking at a certain height level.

© 2021. The Authors.

This is an open access article under the terms of the [Creative Commons Attribution-NonCommercial License](https://creativecommons.org/licenses/by-nc/4.0/), which permits use, distribution and reproduction in any medium, provided the original work is properly cited and is not used for commercial purposes.

The MSU (AMSU) channel 2 (5) at 53.74 GHz (53.595 GHz) measures temperatures in the mid-troposphere (TMT), a layer from the Earth's surface to about 17 km above with its weighting function peaking at about 4 km. The unique feature of the MSU/AMSU measurements is that they provide global coverage without being affected by clouds. As such, they were extensively used for investigating global atmospheric temperature trends and verifying climate model simulations of climate change during the satellite era from 1979 to present (e.g., McKittrick & Christy, 2020; Santer, Fyfe et al., 2017; Santer, Solomon et al., 2017; Santer et al., 2018, 2019).

Several research groups had developed TMT time series, including the NOAA/Center for Satellite Applications and Research (STAR, Zou & Wang, 2011; Zou et al., 2006), the Remote Sensing Systems (RSS, Mears & Wentz, 2009, 2016, 2017; Mears et al., 2003), the University of Alabama at Huntsville (UAH, Christy et al., 2000, 2003; Spencer & Christy, 1992a; Spencer et al., 2017), and the University of Washington (Po-Chedley et al., 2015). These TMT time series were generated by merging similar microwave sounder observations onboard multiple satellites with overlaps. Uncertainties exist in the merged time series and its resulting atmospheric temperature trends, which were mainly caused by instrument calibration drifting errors over time (Christy et al., 2000; Zou & Wang, 2011; Zou et al., 2006), the influence of the instrument body temperature on the measured radiance (e.g., Christy et al., 2000; Mears et al. 2003; Po-Chedley & Fu, 2012, 2013; Zou et al. 2006), diurnal sampling drifting errors owing to satellite orbital drifts (Mears et al., 2003; Po-Chedley et al., 2015; Trenberth & Hurrell, 1997), channel frequency differences between different generations of satellite microwave sounders (Mears & Wentz, 2016; Po-Chedley et al., 2015; Zou & Wang, 2011), and stratospheric cooling effect in TMT (Fu & Johanson, 2005; Fu et al. 2004; Spencer & Christy, 1992b; Wentz & Schabel, 1998). The origination of these errors and how they influence tropospheric temperature trends are summarized in detail in Zou et al. (2018). Imperfect or incorrect corrections of these errors in the satellite merging processes resulted in uncertainties in the derived atmospheric temperature trends, which further caused a global warming debate, especially when they were compared to model simulations of climate changes (e.g., Santer, Fyfe et al., 2017; Santer, Solomon et al., 2017; McKittrick & Christy, 2020). Studies had shown that simulations from both the Coupled Model Intercomparison Project Phase 5 (CMIP5) and 6 (CMIP6) models exhibited TMT warming trends substantially larger than satellite observations (Santer, Fyfe et al., 2017; Santer, Solomon et al., 2017; McKittrick & Christy, 2020). In specific, the global mean TMT warming trends from the ensemble mean of CMIP6 model simulations were larger than satellite observations by a factor of 2 during 1979–2014 (McKittrick & Christy, 2020). The trend disagreement between climate model simulations and satellite observations were particularly large in the 21st century which could be partly attributed to the climate natural variability (Po-Chedley et al., 2021) and possible deficiencies in the post-millennium external forcings used in the model simulations (Santer, Fyfe et al., 2017). New evidence, however, also calls for further investigation and improvement of the satellite observations. Clausius-Clapeyron law poses a physical constraint on the ratio of tropical total column water vapor trends to atmospheric temperature trends (Mears et al. 2007; O’Gorman & Muller, 2010; Wentz & Schabel, 2000). Such constraint was very well maintained by both CMIP5 and CMIP6 model simulations (Santer et al., 2021). However, the satellite observed values of this ratio differs from model simulations by a factor spread as large as 2, depending on satellite data products used from different research groups (Santer et al., 2021). Such a comparison suggested that either the satellite-observed water vapor or tropospheric temperature or both might still contain large errors in climate trend detection. More accurate satellite water vapor and TMT data sets are required for reliable trend detection.

Our goal here is to develop a post-millennium TMT time series using advanced microwave sounder observations on polar-orbiting satellites in stable orbits. In a previous investigation, Zou et al. (2018) suggested that microwave sounder observations of individual satellites in stable orbits had achieved high radiometric stability performance within 0.04 K/Decade for most channels. Here we merge these satellite observations in stable orbits together. With stable orbits, these observations do not incur diurnal drifting errors. In addition, we use channel observations with exactly the same frequency on different satellites, eliminating possible errors owing to frequency differences. With appropriate overlaps, the resulting merged time series achieves an accuracy in trend detection better than 0.012 K/Decade. Global Climate Observing System (GCOS, 2016) recommends that measurement stability for deep layer temperatures should be better than 0.02 K/Decade for climate trend detection with high reliability. The TMT time series developed here exceeds the GCOS stability requirements. As a result, this time series can be used as a reference measurement for climate

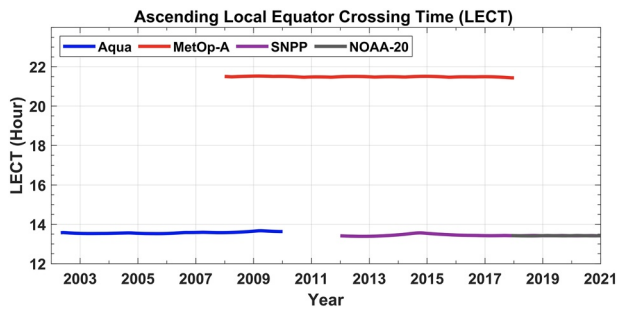


Figure 1. Ascending Local Equator Crossing Time (LECT) for MetOp-A (red), Aqua (blue), Suomi National Polar-orbiting Partnership (S-NPP [purple]), and NOAA Joint Polar Satellite System-1 (NOAA-20 [gray]) polar-orbiting satellites. The descending LECT is 12 h apart from the ascending LECT. The data periods used in this study are 08/2002–12/2009 for Aqua, 01/2008–12/2017 for MetOp-A, 01/2012–12/2020 for S-NPP, and 01/2018–12/2020 for NOAA-20. The S-NPP time series is overlaid by NOAA-20 during their overlapping period.

satellites with their ascending Local Equator Crossing Time (LECT) and descending LECT fixed at close to 1:30 p.m. and 1:30 a.m., respectively (Figure 1). The MetOp-A is a morning satellite with its ascending LECT and descending LECT fixed at close to 9:30 p.m. and 9:30 a.m., respectively (Figure 1). The launch times of these satellites were May 4, 2002 for Aqua, October 19, 2006 for MetOp-A, October 28, 2011 for S-NPP, and November 18, 2017 for NOAA-20. Their overlaps allow construction of a continuous time series. Our starting point for developing the TMT time series is a global monthly brightness temperature (BT) data set with a 2.5° by 2.5° latitude/longitude grid resolution on ascending and descending orbits for each satellite. The conversions from satellite swath radiance observations to gridded data sets are described in the Supporting Information.

3. The Merged TMT Time Series and its Trends

We are interested in the deseasonalized BT anomalies which are defined as BT minus its monthly climatology for the ascending and descending orbits for each satellite. Figure 2 shows the global mean anomaly difference time series between ascending and descending orbits for the four satellites, where the monthly climatology was calculated from the entire observation periods for each satellite. The means of the anomaly differences are exactly zero by their definition, with a standard deviation of 0.007–0.012 K. The trends of anomaly differences are less than 0.01 K/Decade that are statistically insignificant for the three satellites with longer observations. The trend for NOAA-20 is slightly larger due to short observations, but it is also statistically insignificant. With little differences, the ascending and descending anomalies were averaged to give the daily mean anomalies for each satellite.

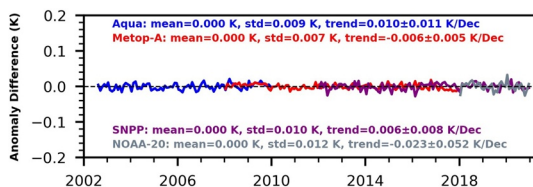


Figure 2. Global mean brightness temperature anomaly differences between ascending and descending orbits. The differences are for ascending minus descending (1:30 p.m. minus 1:30 a.m.) for Aqua (blue), Suomi National Polar-orbiting Partnership (S-NPP, purple) and NOAA Joint Polar Satellite System-1 (NOAA-20, gray) and descending minus ascending (9:30 a.m. minus 9:30 p.m.) for MetOp-A (red). The anomalies are relative to the monthly climatology calculated for the entire observation periods for each satellite.

trend detection and verifying climate model simulations of atmospheric temperature trends. We provide global TMT trends for the period from 2002 to 2020 and compare with those from existing data sets developed by different research groups. We show that the existing versions of TMT time series developed including satellites with orbital drifts contain drifting errors and underestimate the tropospheric warming by about 14%.

2. Satellites and Instruments

We use the AMSU channel 5 observations onboard NASA's Aqua and EUMETSAT MetOp-A satellites, and the Advanced Technology Microwave Sounder (ATMS) channel 6 (also 53.596 GHz) observations onboard the NOAA/NASA Suomi National Polar-orbiting Partnership (S-NPP) and onboard the NOAA Joint Polar Satellite System-1 (JPSS-1, renamed NOAA-20 after launch) satellites to develop the TMT time series. The AMSU are the second and ATMS the third generations of satellite microwave sounders following the MSU. A detailed description on the instrument characteristics and data processing approaches are provided in the Supporting Information. The Aqua, S-NPP and NOAA-20 are afternoon

satellites with their ascending Local Equator Crossing Time (LECT) and descending LECT fixed at close to 1:30 p.m. and 1:30 a.m., respectively (Figure 1). The MetOp-A is a morning satellite with its ascending LECT and descending LECT fixed at close to 9:30 p.m. and 9:30 a.m., respectively (Figure 1). The launch times of these satellites were May 4, 2002 for Aqua, October 19, 2006 for MetOp-A, October 28, 2011 for S-NPP, and November 18, 2017 for NOAA-20. Their overlaps allow construction of a continuous time series. Our starting point for developing the TMT time series is a global monthly brightness temperature (BT) data set with a 2.5° by 2.5° latitude/longitude grid resolution on ascending and descending orbits for each satellite. The conversions from satellite swath radiance observations to gridded data sets are described in the Supporting Information. With little differences, the ascending and descending anomalies were averaged to give the daily mean anomalies for each satellite. To merge the BT anomalies from different satellites, we need to make an adjustment so that the BT anomalies of individual satellites are defined relative to the same monthly climatology. We take the MetOp-A monthly climatology as a reference and adjust the Aqua and S-NPP anomalies by subtracting a “monthly climatology” of the anomaly differences relative to MetOp-A during their overlapping periods. We then adjust NOAA-20 to the adjusted S-NPP using their overlaps. After this adjustment, the anomalies from the four satellites are merged together to generate a TMT time series for the entire 2002–2020 period for trend investigation.

Figure 3a shows the global mean anomaly time series of individual satellites as well as the merged time series, which is the average of two satellite observations during overlapping periods, and Figure 3b shows

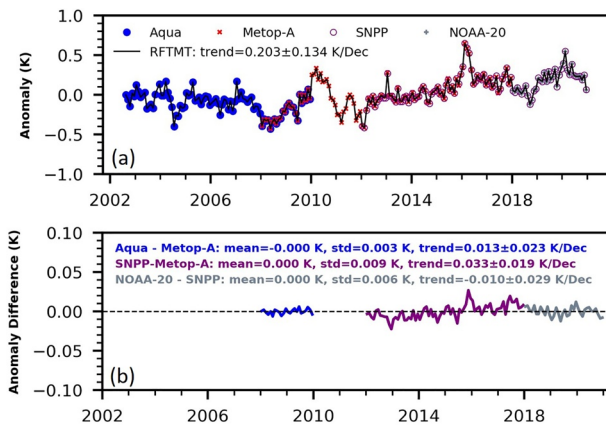


Figure 3. (a) Monthly global mean temperatures in the mid-troposphere (TMT) anomaly time series from Aqua, MetOp-A, Suomi National Polar-orbiting Partnership (S-NPP), and NOAA Joint Polar Satellite System-1 (NOAA-20) and the reference TMT (RFTMT) time series merged from these satellites; (b) inter-satellite difference time series before the merging. Anomalies are relative to a monthly climatology of RFTMT for the MetOp-A period from January 2008 to December 2017. Uncertainties in trend calculations represent 95% confidence intervals with autocorrelation adjustments.

inter-satellite difference time series for relevant satellite pairs. The maximum trend seen in the inter-satellite differences is from the MetOp-A and S-NPP pair, being 0.033 K/Decade. Since there are no diurnal drifting errors and channel frequencies are identical for different satellites, this difference trend only represents relative drifts over time in calibration biases between MetOp-A and S-NPP. Calibration drifts over time are likely caused by instrument degradation. Specific mechanisms in instrument degradation causing this bias drift are unknown yet, but they may include changes in instrument amplifier nonlinearity (Zou & Wang, 2011), changes in side lobe efficiency due to instrument reflector degradation (Obligis et al., 2007), and measurement leakage incurred when the instrument antenna switches between the Earth view and calibration target views (Ruf, 2002). When satellites were calibrated independently, as used in this study, it is unlikely that their biases were drifting to the same direction to arrive at a small relative drifting error. As such, Zou et al. (2018) suggested that the relative drifting errors between satellite pairs in stable orbits shall represent the radiometric stability of individual satellite observations. In a comprehensive assessment of inter-satellite difference time series for satellite pairs in stable orbits, Zou et al. (2018) found that most ATMS channels onboard S-NPP and AMSU channels onboard MetOp-A and Aqua achieved a radiometric stability within 0.04 K/Decade. The radiometric stability found here (0.033 K/Decade) for the MetOp-A and S-NPP TMT channel is consistent with those found in Zou et al. (2018). The required stability for deep layer temperatures to reliably

detect climate trends is 0.02 K/Decade (GCOS, 2016). Consequently, the radiometric stability of TMT channel for individual satellites are larger than the required measurement stability.

After satellite merging, however, the measurement stability of the averaged trends would become smaller than the radiometric stability of individual satellites. Based on the measurement error analysis with small sampling size (e.g., Bell, 1999), the uncertainty of the averaged trends after satellite merging is expressed as $\pm \frac{\Delta}{2\sqrt{N}}$, where Δ ($=0.033$ K/Decade) denotes the maximum relative drifting error, or spread of trends, and N ($=2$) the number of overlapping satellites. Note that the uncertainty of the averaged trends is determined only by the maximum relative drifting error and the number of overlapping satellites, regardless of the radiometric stabilities of individual satellites. The underlying assumption for this uncertainty expression is that uncertainty in a single measurement equals one-half of the spread. This results in a trend uncertainty, or stability, of only 0.012 K/Decade for the merged time series over periods with satellite overlaps. By assuming that a satellite without overlaps (Figure 3a) has a drifting error of 0.033 K/Decade while each of the two overlapping satellites has one-half of this drifting error, we obtained a trend uncertainty also of 0.012 K/Decade for the entire observation period of the merged time series based on statistical simulations.

Owing to its high accuracy, the merged TMT time series developed here can be considered as a reference measurement, abbreviated as RFTMT, for the variability and trend detection. The RFTMT trend in Figure 3a is 0.203 K/Decade, with a 95% confidence interval of ± 0.134 K/Decade, during 2002–2020, where the confidence interval was calculated with autocorrelation adjustments (Wigley, 2006). Note that the measurement uncertainty of trends as discussed above is different from the statistical uncertainty, or confidence interval, which is associated with the length and variability of a time series in trend calculations. Statistical uncertainty would typically be larger but become smaller as observations become longer (Wigley, 2006).

Based on its weighting function distribution, the global mean TMT trend contains about 13% of contribution from the lower-stratosphere and 87% of contribution from the bulk tropospheric layer from the Earth's surface to about 10 km (See the Supporting Information). During 2002–2020, the lower-stratospheric temperature trend was close to zero (Supporting Information) and thus had negligible contribution to the TMT trend. This gives an actual tropospheric temperature trend of 15% ($=1/0.87-1$) higher than the TMT trend, being 0.230 K/Decade with a 95% confidence interval of ± 0.134 K/Decade. When only the measurement

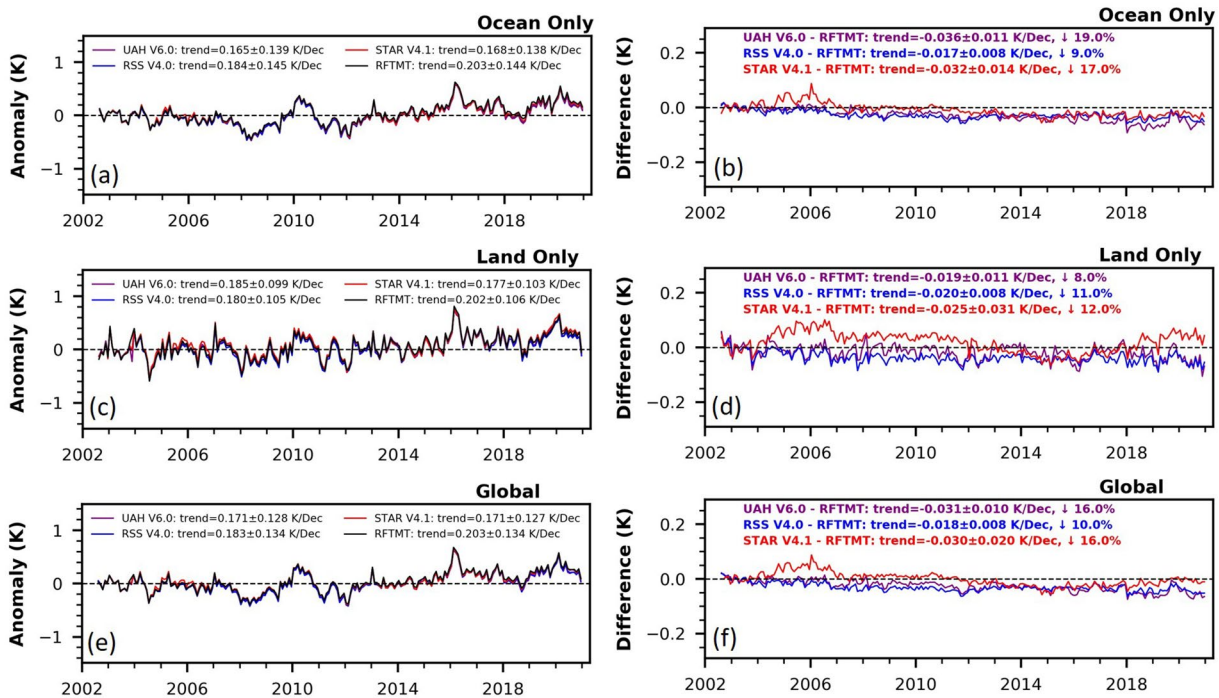


Figure 4. Comparisons of temperatures in the mid-troposphere (TMT) time series between existing data sets and reference TMT (RFTMT) from the present study during August 2002–December 2020. (a) TMT monthly anomalies averaged over the global ocean; (b) Anomaly difference time series between existing data sets and RFTMT over the global ocean; (c) TMT monthly anomalies averaged over the global land; (d) Anomaly difference time series between existing data sets and RFTMT over the global land; (e) Global-mean TMT monthly anomalies; (f) Global-mean anomaly difference time series between existing datasets and RFTMT. Time series are plotted so that their mean differences during 08/2002–12/2003 are zero.

uncertainty is considered, this trend translates to a total tropospheric warming of 0.420 ± 0.022 K during 2002–2020.

4. Comparisons With Other Satellite-Based TMT Time Series

Figure 4 compares the existing TMT data sets from STAR V4.1, RSS 4.0, and UAH V6.0 over ocean and land and globe (see the Supporting Information for a description of the existing data sets) with RFTMT. As seen, different versions of the anomaly time series show excellent agreement in variability (Figures 4a, 4c and 4e). This is expected since all of these data sets used channels with the same frequency that have the same sensitivity to TMT changes. The main feature in the comparison is that RFTMT has warming trends larger than all of the existing data sets over both ocean and land by a range from the smallest 0.019 K/Decade (8%) for UAH over land to the largest 0.036 K/Decade (19%) for UAH over ocean, which are all statistically significant. The global mean trends of RSS, STAR, and UAH are biased cool by 0.018 K/Decade (10%), 0.030 K/Decade (16%), and 0.031 K/Decade (16%), respectively (Figure 4f). The uncertainty in TMT trends that includes diurnal drifting errors is typically 0.042 K/Decade, determined by Monte Carlo approach (Mears et al., 2011). The cool biases in trends in the three data sets examined here are all within this range of uncertainty. By average, the global mean warming rate from STAR, RSS, and UAH is 0.175 K/Decade, 14% lower than that from the RFTMT during 08/2002–12/2020.

The difference time series between the existing data sets and RFTMT over ocean (Figure 4b) and land (Figure 4d) provided clues on how their trend differences occurred. Over the ocean, all existing data sets show downward trends relative to RFTMT during 2002–2020, except that the STAR data had a warming spike for a few years before 2006 (Figure 4b). Diurnal drift corrections may cause trend uncertainties in the existing data sets on the order of 0.02 K/Decade over the ocean (Po-Chedley et al., 2015). However, since diurnal drift-related uncertainties are of random nature in different data sets, the common downward trends in STAR, RSS, and UAH relative to RFTMT can be most likely attributed to a common cause—calibration

drifting errors in NOAA-15 used in those data sets. It is known that NOAA-15 AMSU channel 5 had a large cooling drift at least in its later period of operations (Mears & Wentz, 2016; Mears et al., 2011; Spencer et al., 2017). The use of NOAA-15 observations in STAR V4.1 until August 2015 could explain its cooling trend relative to RFTMT. The RSS and UAH used NOAA-15 observations from close to its launch time to 2010 and 2007, respectively (Mears & Wentz, 2016; Spencer et al., 2017). Cooling drifts in NOAA-15 before these cut-off years may still have affected trends and caused their overall cooling biases relative to the RFTMT.

The RSS data over land shows a cooling trend relative to RFTMT very similar to that over ocean (Figure 4d), which may suggest that its diurnal drift correction algorithms perform well over land. The UAH time series over land is much closer to the RFTMT than over ocean, suggesting an overcorrection of the diurnal drifting errors over land. The STAR time series over land wiggles relative to RFTMT, suggesting some inconsistencies in diurnal drift corrections. This will be improved in the STAR Version 5.0 that is being developed.

5. Discussion

We have developed a TMT time series using satellites only in stable orbits and propose to use it as a reference measurement in climate trend detection. This RFTMT achieves an accuracy of 0.012 K/Decade in climate trend detection, higher than the measurement stability requirement of 0.02 K/Decade as recommended by GCOS (2016). In comparisons to the existing TMT time series developed from satellites with orbital drifts, the error structure of RFTMT is relatively simpler with smaller uncertainties in climate trend detection. This makes RFTMT a complement to the existing TMT products, although observation period of the former is shorter than the later. There are several benefits in using RFTMT in climate change investigations. First, with better accuracy, the RFTMT is expected to help understand and reconcile trend differences between different data sets. In specific, RFTMT could be used as a reference to recalibrate satellites with orbital drifts and in development of diurnal correction algorithms in future development of TMT time series. Such an application may improve the accuracy of TMT time series with longer observation periods. Second, the merging approach for developing RFTMT could be extended to other channels in microwave sounder observations, allowing development of temperature time series from the mid-troposphere to the upper stratosphere for studies of vertical structure in trends with better accuracy. As an example, post-millennium reference layer mean temperature time series of the lower-stratosphere has already been developed by merging AMSU channel 9 and ATMS channel 10 using satellites only with stable orbits (not shown). Third, RFTMT could be used to examine trends from climate model simulations with better accuracy. This will help explore the role of climate natural variability and identify possible defects in climate model simulations with higher confidence which will in turn lead to development of better climate models for improved climate simulations and predictions.

The current RFTMT includes only four polar-orbiting satellites with stable orbits. Other available satellites in stable orbits could also be added to the time series for a sustained monitoring of the tropospheric temperature trends. These may include MetOp-C that is also a 9:30 a.m. morning satellite in the MetOp series. Owing to a gain jump found on October 17, 2016 in the MetOp-B AMSU instrument (See Supporting Information), however, MetOp-B was not used in this study, although it has longer observations in stable orbits. Recalibration aiming at removing bias jumps in BTs caused by gain jumps is needed before MetOp-B can be used in the RFTMT time series for trend detection with high accuracy. Future JPSS satellites that will carry the ATMS instrument are all planned to be launched onto the same stable afternoon orbit as S-NPP and NOAA-20 in the next 15 years. These satellites will allow the RFTMT time series to extend into the next two decades and beyond. Furthermore, adding those satellites could also be helpful in filling possible gaps in time series and further reducing uncertainties in trend monitoring.

Data Availability Statement

The reference TMT data developed in this study are available from the NOAA/STAR website: <https://www.star.nesdis.noaa.gov/smcd/emb/mscat/products.php>. We have used AMSU-A L1c data onboard Aqua and MetOp-A and ATMS L1c data onboard S-NPP and NOAA-20 in this study. The Aqua AMSU-A L1c data are accessible from the NASA GES DISC Data Archive website: <https://airs11.gesdisc.eosdis.nasa.gov/data/>

[Aqua_AIRS_Level1/AIRABRAD.005/](#). The MetOp-A AMSU-A L1c data are accessible from the NOAA/NCEI Climate Data Record Program: <https://www.ncdc.noaa.gov/cdr/fundamental>.

Acknowledgments

We thank the anonymous reviewers for helpful comments. The work was supported by the NOAA/Joint Polar Satellite System (JPSS) Proving Ground and Risk Reduction Program and the NOAA/Climate Program Office Program, NOAA-OAR-CPO-2018-2005133-OOM, and NOAA Grant NA18OAR4310423. The views, opinions, and findings contained in this report are those of the authors and should not be construed as an official NOAA or U.S. Government position, policy, or decision.

References

- Bell, S. A. (1999). *Beginner's guide to uncertainty of measurement*, Issue 2 (p. 33). Middlesex, United Kingdom: National Physical Laboratory Teddington. ISSN 1368-6550.
- Christy, J. R., Spencer, R. W., & Braswell, W. D. (2000). MSU tropospheric temperatures: Dataset construction and radiosonde comparisons. *Journal of Atmospheric and Oceanic Technology*, *17*, 1153–1170. [https://doi.org/10.1175/1520-0426\(2000\)017<1153:mttdca>2.0.co;2](https://doi.org/10.1175/1520-0426(2000)017<1153:mttdca>2.0.co;2)
- Christy, J. R., Spencer, R. W., Norris, W. B., Braswell, W. D., & Parker, D. E. (2003). Error estimates of version 5.0 of MSU-AMSU bulk atmospheric temperature. *Journal of Atmospheric and Oceanic Technology*, *20*, 613–629. [https://doi.org/10.1175/1520-0426\(2003\)20<613:eeovom>2.0.co;2](https://doi.org/10.1175/1520-0426(2003)20<613:eeovom>2.0.co;2)
- Fu, Q., & Johanson, C. M. (2005). Satellite-derived vertical dependence of tropical tropospheric temperature trends. *Geophysical Research Letters*, *32*, L10703. <https://doi.org/10.1029/2004gl022266>
- Fu, Q., Johanson, C. M., Warren, S. G., & Seidel, D. J. (2004). Contribution of stratospheric cooling to satellite-inferred tropospheric trends. *Nature*, *429*, 55–58. <https://doi.org/10.1038/nature02524>
- GCOS/WMO (2016). *The Global Observing System for Climate: Implementation needs, GCOS- 200 (GOOS-214)* (p. 341). Switzerland: World Meteorological Organization.
- Kidwell, K. B. (1998). NOAA polar orbiter data users guide. NOAA. Retrieved from http://webapp1.dlib.indiana.edu/virtual_disk_library/index.cgi/4284724/FID2496/podug/index.htm
- McKittrick, R., & Christy, J. R. (2020). Pervasive warming bias in CMIP6 tropospheric layers. *Earth and Space Science*, *7*, e2020EA001281. <https://doi.org/10.1029/2020ea001281>
- Mears, C. A., Santer, B. D., Wentz, F. J., Taylor, K. E., & Wehner, M. (2007). The relationship between temperature and precipitable water changes over tropical oceans. *Geophysical Research Letters*, *34*, L24709. <https://doi.org/10.1029/2007gl031936>
- Mears, C. A., Schabel, M. C., & Wentz, F. J. (2003). A reanalysis of the MSU channel 2 tropospheric temperature record. *Journal of Climate*, *16*, 3650–3664. [https://doi.org/10.1175/1520-0442\(2003\)016<3650:arotmc>2.0.co;2](https://doi.org/10.1175/1520-0442(2003)016<3650:arotmc>2.0.co;2)
- Mears, C. A., & Wentz, F. J. (2009). Construction of the remote sensing systems v3.2 atmospheric temperature records from the MSU and AMSU microwave sounders. *Journal of Atmospheric and Oceanic Technology*, *26*, 1040–1056. <https://doi.org/10.1175/2008jtecha1176.1>
- Mears, C. A., & Wentz, F. J. (2016). Sensitivity of satellite-derived tropospheric temperature trends to the diurnal cycle adjustment. *Journal of Climate*, *29*, 3629–3646. <https://doi.org/10.1175/jcli-d-15-0744.1>
- Mears, C. A., & Wentz, F. J. (2017). A satellite-derived lower-tropospheric atmospheric temperature dataset using an optimized adjustment for diurnal effects. *Journal of Climate*, *30*(19), 7695–7718. <https://doi.org/10.1175/jcli-d-16-0768.1>
- Mears, C. A., Wentz, F. J., Thone, P., & Bernie, D. (2011). Assessing uncertainty in estimates of atmospheric temperature changes from MSU and AMSU using a Monte-Carlo estimation technique. *Journal of Geophysical Research*, *116*, D08112. <https://doi.org/10.1029/2010jd014954>
- Obligis, E., Eymard, L., & Tran, N. (2007). A new sidelobe correction algorithm for microwave radiometers: Application to the Envisat instrument. *IEEE Transactions on Geoscience and Remote Sensing*, *45*(3), 602–612. <https://doi.org/10.1109/tgrs.2006.887165>
- O’Gorman, P. A., & Muller, C. J. (2010). How closely do changes in surface and column water vapor follow Clausius-Clapeyron scaling in climate change simulations? *Environmental Research Letters*, *5*, 025207.
- Po-Chedley, S., & Fu, Q. (2012). A bias in the midtropospheric channel warm target factor on the NOAA-9 microwave sounding unit. *Journal of Atmospheric and Oceanic Technology*, *29*, 646–652. <https://doi.org/10.1175/JTECH-D-11-00147.1>
- Po-Chedley, S., & Fu, Q. (2013). Reply to “Comments on ‘A bias in the midtropospheric channel warm target factor on the NOAA-9 microwave sounding unit’”. *Journal of Atmospheric and Oceanic Technology*, *30*, 1014–1020. <https://doi.org/10.1175/JTECH-D-12-00131.1>
- Po-Chedley, S., Santer, B. D., Fueglistaler, S., Zelinka, M. D., Cameron-Smith, P. J., Painter, J. F., & Fu, Q. (2021). Natural variability contributes to model-satellite differences in Tropical tropospheric warming. *Proceedings of the National Academy of Sciences of the United States of America*, *118*(13), e2020962118. <https://doi.org/10.1073/pnas.2020962118>
- Po-Chedley, S., Thorsen, T. J., & Fu, Q. (2015). Removing diurnal cycle contamination in satellite derived tropospheric temperatures: Understanding tropical tropospheric trend discrepancies. *Journal of Climate*, *28*, 2274–2290. <https://doi.org/10.1175/jcli-d-13-00767.1>
- Ruf, C. S. (2002). Characterization and correction of a drift in calibration of the TOPEX microwave radiometer. *IEEE Transactions on Geoscience and Remote Sensing*, *40*(2), 509–511. <https://doi.org/10.1109/36.992824>
- Santer, B. D., Bonfils, C. J. W., Fu, Q., Fyfe, J. C., Hegerl, G. C., Mears, C., et al. (2019). Celebrating the anniversary of three key events in climate change Science. *Nature Climate Change*, *9*(3), 180–182. <https://doi.org/10.1038/s41558-019-0424-x>
- Santer, B. D., Fyfe, J. C., Pallotta, G., Flato, G. M., Meehl, G. A., England, M. H., et al. (2017). Causes of differences in model and satellite tropospheric warming rates. *Nature Geoscience*, *10*, 478–485. <https://doi.org/10.1038/ngeo2973>
- Santer, B. D., Po-Chedley, S., Mears, C., Fyfe, J. C., Gillett, N., Fu, Q., et al. (2021). Using climate model simulations to constrain observations. *Journal of Climate*, *1*, 59. <https://doi.org/10.1175/JCLI-D-20-0768.1>
- Santer, B. D., Po-Chedley, S., Zelinka, M. D., Cvijanovic, I., Bonfils, C., Durack, P. J., et al. (2018). Human influence on the seasonal cycle of tropospheric temperature. *Science*, *361*(6399), eaas8806. <https://doi.org/10.1126/science.aas8806>
- Santer, B. D., Solomon, S., Pallotta, G., Mears, C., Po-Chedley, S., Fu, Q., et al. (2017). Comparing tropospheric warming in climate models and satellite data. *Journal of Climate*, *30*, 373–392. <https://doi.org/10.1175/jcli-d-16-0333.1>
- Spencer, R. W., & Christy, J. R. (1992a). Precision and radiosonde validation of satellite gridpoint temperature anomalies Part I: MSU channel 2. *Journal of Climate*, *5*, 847–857. [https://doi.org/10.1175/1520-0442\(1992\)005<0847:parvos>2.0.co;2](https://doi.org/10.1175/1520-0442(1992)005<0847:parvos>2.0.co;2)
- Spencer, R. W., & Christy, J. R. (1992b). Precision and radiosonde validation of satellite gridpoint temperature anomalies. Part II: Tropospheric retrieval and trends during 1979–90. *Journal of Climate*, *5*, 858–866. [https://doi.org/10.1175/1520-0442\(1992\)005<0858:parvos>2.0.co;2](https://doi.org/10.1175/1520-0442(1992)005<0858:parvos>2.0.co;2)
- Spencer, R. W., Christy, J. R., & Braswell, W. D. (2017). UAH version 6 global satellite temperature products: Methodology and results. *Asia-Pacific Journal of Atmospheric Sciences*, *53*, 121–130. <https://doi.org/10.1007/s13143-017-0010-y>
- Trenberth, K. E., & Hurrell, J. W. (1997). How accurate are satellite ‘thermometers’? *Nature*, *389*, 342. <https://doi.org/10.1038/38640-c1>
- Wentz, F. J., & Schabel, M. C. (1998). Effects of satellite orbital decay on satellite-derived lower-tropospheric temperature trends. *Nature*, *394*, 661–664. <https://doi.org/10.1038/292267>

- Wentz, F. J., & Schabel, M. C. (2000). Precise climate monitoring using complementary satellite data sets. *Nature*, *403*, 414–416. <https://doi.org/10.1038/35000184>
- Wigley, T. M. L. (2006). Statistical Issues Regarding Trends. In T. R. Karl, S. J. Hassol, C. D. Miller, & W. L. Murray (Eds.), *Temperature trends in the lower atmosphere: Steps for understanding and reconciling differences*. Washington, D. C. Retrieved from <https://www.globalchange.gov/browse/reports/sap-11-temperature-trends-lower-atmosphere-steps-understanding-reconciling>
- Zou, C.-Z., Goldberg, M., Cheng, Z., Grody, N. C., Sullivan, J. T., Cao, C., & Tarpley, D. (2006). Recalibration of microwave sounding unit for climate studies using simultaneous nadir overpasses. *Journal of Geophysical Research*, *111*, D19114. <https://doi.org/10.1029/2005jd006798>
- Zou, C.-Z., Goldberg, M., & Hao, X. (2018). New generation of U.S. satellite microwave sounder achieves high radiometric stability performance for reliable climate change detection. *Science Advances*, *4*(10), eaau0049. <https://doi.org/10.1126/sciadv.aau0049>
- Zou, C.-Z., & Wang, W. (2011). Inter-satellite calibration of AMSU-A observations for weather and climate applications. *Journal of Geophysical Research*, *116*, D23113. <https://doi.org/10.1029/2011jd016205>

References From the Supporting Information

- Gelaro, R., McCarty, W., Suárez, M. J., Todling, R., Molod, A., Takacs, L., et al. (2017). The modern-era retrospective analysis for research and applications, version 2 (MERRA-2). *Journal of Climate*, *30*(14), 5419–5454.
- Han, Y., vanDelst, P., Liu, Q., Weng, F., Yan, B., Treadon, R., & Derber, J. (2006). *JCSDA community radiative transfer model (CRTM)–Version 1*. NOAA Tech. Rep. NESDIS (Vol. 122, p. 40). Natl. Oceanic and Atmos. Admin, Silver Spring, Md.
- JPL AIRS Project (2000). *Algorithm theoretical basis document level 1b, Part 3: Microwave instruments. Version 2.1* (p. 53). JPL D-17005.
- JPL AIRS Project Instrument Suite (2020). Retrieved from <https://airs.jpl.nasa.gov/mission/instrument/amsu-a-and-hsb/>
- NOAA STAR Integrated Calibration/Validation System (2021). Retrieved from <https://www.star.nesdis.noaa.gov/icvs/index.php>
- Wang, W., & Zou, C.-Z. (2014). AMSU-A-only atmospheric temperature data records from the lower troposphere to the top of the stratosphere. *Journal of Atmospheric and Oceanic Technology*, *31*, 808–825.
- Weng, F., Zou, X., Sun, N., Yang, H., Tian, M., Blackwell, W. J., et al. (2013). Calibration of Suomi national polar-orbiting partnership advanced technology microwave sounder. *Journal of Geophysical Research: Atmosphere*, *118*, 11187–11200. <https://doi.org/10.1002/jgrd.50840>
- Zhang, K., Zhou, L., Goldberg, M., Liu, X., Wolf, W., Tan, C., & Liu, Q. (2017). A methodology to adjust ATMS observations for limb effect and its applications. *Journal of Geophysical Research: Atmosphere*, *122*, 11347–11356. <https://doi.org/10.1002/2017JD026820>
- Zou, C.-Z., Zhou, L., Lin, L., Sun, N., Chen, Y., Flynn, L. E., et al. (2020). The reprocessed Suomi NPP satellite observations. *Remote Sensing*, *12*(18), 2891.
- Zou, X., Weng, F., & Yang, H. (2014). Connecting the time series of microwave sounding observations from AMSU to ATMS for long-term monitoring of climate. *Journal of Atmospheric and Oceanic Technology*, *31*, 2206–2222.